JOURNAL OF GEOPHYSICAL RESEARCH, VOL. 101, NO. D1, PAGES 1763–1778, JANUARY 20, 1996

Three-dimensional distribution of nonmenthane hydrocarbons and halocarbons over the northwestern Pacific during the 1991 Pacific Exploratory Mission (PEM-West A)

Donald R. Blake, Tai-Yih Chen, Tyrrel W. Smith Jr.[1], Charles J.-L. Wang[2],

Oliver W. Wingenter, Nicola J. Blake, and F. S. Rowland

Department of Chemistry, University of California, Irvine

Edward W. Mayer[3]

Department of Chemistry, U.S. Military Academy, West Point, New York

Abstract. A total of 1667 whole air samples were collected onboard the NASA DC-8 aircraft during the 6-week Pacific Exploratory Mission over the western Pacific (PEM-West A) in September and October 1991. The samples were assayed for 15 C_2-C_7 hydrocarbons and six halocarbons. Latitudinal (0.5°S to 59.5°N) and longitudinal (114°E to 122°W) profiles were obtained from samples collected between ground level and 12.7 km. Thirteen of the 18 missions exhibited at least one vertical profile where the hydrocarbon mixing ratios increased with altitude. Longitude-latitude color patch plots at three altitude levels and three-dimensional color latitude-altitude and longitude-altitude contour plots exhibit a significant number of middle-upper tropospheric pollution events. These and several lower tropospheric pollution plumes were characterized by comparison with urban data from Tokyo and Hong Kong, as well as with natural gas and the products from incomplete combustion. Elevated levels of nonmethane hydrocarbons (NMHC) and other trace gases in the upper-middle free troposphere were attributed to deep convection over the Asian continent and to typhoon-driven convection near the western Pacific coast of Asia. In addition, NMHCs and CH_3CCl_3 were found to be useful tracers with which to distinguish hydrocarbon and halocarbon augmented plumes emitted from coastal Asian cities into the northwestern Pacific.

Introduction

Nonmethane hydrocarbons (NMHCs) and halocarbons affect both tropospheric and stratospheric photochemistry. The sources of these atmospheric trace species are predominantly land based and the main mechanism for the removal of those hydrocarbons and halocarbons with abstractable hydrogen atoms is through oxidative reaction with hydroxyl radicals (OH) as in (1).

$$RH + HO\cdot \rightarrow R\cdot + H_2O \quad (1)$$

Nonmethane hydrocarbon emission patterns can be used to characterize anthropogenic sources such as fossil fuel leakage and incomplete combustion [*Ehhalt and Rudolph*, 1984; *Blake et al.*, 1992, 1994, 1995; *Smith*, 1993]. Because all of the halocarbons reported here are anthropogenic and released predominantly in cities, their measurement can be used to estimate recent urban influence on an air mass. For example, an air parcel which has been augmented by biomass burning would be expected to contain elevated levels of ethane, ethene, and ethyne and many other hydrocarbons, while exhibiting no chlorofluorocarbon enhancement [*Crutzen and Andreae*, 1990; *Blake et al.*, 1992, 1994; *Smith*, 1993]. Industrial activity would be indicated by elevated concentrations of chlorofluorocarbons, as well as CCl_4 (carbon tetrachloride), CH_3CCl_3 (methyl chloroform), C_2Cl_4 (perchloroethene), and other halocarbons [*Crutzen*, 1980; *Rasmussen et al.*, 1982; *Blake et al.*, 1992, *Smith;* 1993]. Natural gas emissions are associated with elevated levels of methane, ethane, and other light alkanes with no accompanying halocarbons [*Blake et al.*, 1994].

We report the general results of measurements of 15 saturated and unsaturated C_2-C_7 NMHCs and six halocarbons, namely, CCl_2F_2 (CFC-12), CCl_3F (CFC-11), CCl_2FCClF_2 (CFC-113), CH_3CCl_3, CCl_4, and C_2Cl_4, in air samples collected onboard the NASA DC-8 aircraft between September 7 and October 22, 1991, during NASA's Pacific Exploratory Mission over the western Pacific (PEM-West A). The mission flew from San Jose, California, around the North Pacific rim and back through the central Pacific, with many additional flights from Tokyo, Hong Kong, Guam, and Hawaii. Numerous vertical profiles in the altitude range from 0.3 km to 12.7 km were flown over the ocean, with additional vertical profiles near urban areas during landings. In addition, the meteorological consequences of several typhoon events were encountered during the project, including fast vertical transport associated with Typhoons Nat and Mireille. These flights provided an excellent opportunity to examine the large-scale transport and distribution of NMHCs and halocarbons in the northwestern Pacific region.

[1]Now at Cooperative Institute for Research in Environmental Sciences, University of Colorado, Boulder.

[2]Now at National Central University, Department of Chemistry, Chung-Li, Taiwan 32054 R.O.C.

[3]Now at University of California, San Diego, Department of Chemistry and Biochemistry, La Jolla, California.

Paper number 95JD02707.
0148-0227/96/95JD-02707$05.00

Experiment

Sampling

The whole air sampling apparatus was mounted onboard the NASA DC-8 jet aircraft. The stainless steel 1/4-inch OD inlet and outlet were installed on the port side of the aircraft, forward of the wing section. The gas-handling manifold and the two-stage metal bellows pump (Metal Bellows Company, MB-602), connected in series, were configured to allow the sample canisters to be routinely filled to 40 psig and the system to be operated at pressures up to 60 psig before activation of a pressure relief valve. The 2-L sample canisters were assembled in fixed sets of 24, connected to a single manifold and arranged in three parallel columns of eight canisters. Rack mountings were available on the aircraft for six of these 24-canister sets, allowing a maximum of 144 samples to be collected per flight. These 24-canister sets formed the basic unit for sampling operations onboard the DC-8 and for shipments between the various staging sites and the analytical laboratory, which was assembled in Japan at the Yokota US Air Force Base near Tokyo. Details of sample canister fabrication and filling procedures have been discussed earlier [*Blake et al.*, 1992, 1994; *Smith*, 1993].

The operation of a field laboratory at Yokota Air Base, Japan, one of the main staging sites for this mission, reduced the time required for sample canister transportation between aircraft landing sites and the analytical laboratory. For staging sites other than Yokota the filled sample canister sets were shipped by air cargo on commercial flights to Tokyo and then transported to Yokota. On average, approximately 90 air samples were collected on each flight and analyzed within 7 days. The total number of sample canisters available for the mission was approximately 700, requiring multiple use of canisters to maintain this high sampling frequency. After the air samples from earlier flights had been satisfactorily assayed, the canisters were evacuated to a pressure of 10^{-2} torr and shipped back to the DC-8 for subsequent missions.

Chemical Analysis

Each sample was analyzed for NMHCs and halocarbons using two Hewlett-Packard 5890 series II gas chromatographs (GCs). One gas chromatograph (GC-1), was equipped with two flame ionization detectors (FIDs), while GC-2 was equipped with an electron capture detector (ECD). One of the FIDs monitored the output of a 30 m x 0.53 mm Al_2O_3/KCl PLOT column (J & W Scientific) with a hydrogen carrier flow of 9.5 mL/min and provided data on C_2-C_5 NMHC compounds. A 60 m x 0.25 mm, 0.25-μm film thickness DB-1 column (J & W Scientific) with a hydrogen carrier flow of 2.0 mL/min was installed in the second FID for the purpose of detecting C_3-C_{10} NMHCs. Coupled to the ECD, GC-2 utilized a 50 m x 0.2 mm, 0.5-μm film thickness PONA column (Hewlett-Packard) with a hydrogen carrier flow of 1.2 mL/min for halocarbon separation and detection.

A precise volume of air (1309 mL STP) from each sample canister was trapped in a preconcentration loop (8 inch x 1/4-inch OD, stainless steel) filled with 1-mm-diameter glass beads and immersed in liquid nitrogen. The volatile contents of the sample were pumped off while the higher boiling gases remained on the glass beads. The contents of the loop were voporized by heating with warm water and flushed with the hydrogen carrier gas through a splitter which divided the sample into three separate flow streams. Precisely reproducible percentages of the total flow were injected onto the various columns: 75% to the PLOT column, 15% to the DB-1, and 10% to the PONA. It was found that the sample split was very reproducible if the specific humidity of the sample was greater than 2.0 g H_2O/kg air. Thus to raise the specific humidity of the driest samples, as much as 2.0 torr of purified water was added to the 2119 mL STP volume of the analytical vacuum line prior to sample introduction. Upon sample injection the initial temperature of GC-2 was held at -60°C for 30 s, and then ramped up to 240°C at 20°/min, while the initial temperature of -20°C for GC-1 was ramped up to 200°C at 20°/min. A complete analysis cycle, including return to the cooled initial conditions, required 20 min. The gas chromatographs were interfaced to three Spectra Physics 4400 computing integrators and a computer, using LABNET software (Spectra Physics) for data capture and storage. To monitor the consistency and reproducibility of the analytical system, a secondary standard (dry ambient air collected at Niwot Ridge, Colorado, NOAA CMDL by Paul Steele) was analyzed after every eight ambient samples. Throughout the project a second cylinder of whole air was assayed every other day. These mixing ratios were compared to those obtained from the working standard to ascertain that the working standard mixing ratios did not change over the period of the experiment. Approximately 60 air samples could be analyzed during a 24-hour period. The chromatographic apparatus was run continuously (24 hours/d, 7 days/week) from September 17 to November 2, 1991. Detailed descriptions of the analytical setup, standards and calibrations have been given previously [*Blake et al.*, 1992, 1994]. While data from the integrators provided preliminary concentration values for the reported compounds, after returning to our home laboratory, the chromatograms were examined to confirm that the baselines were correctly drawn and that the peaks showed no unusual characteristics.

The precision of the air sample measurements, based on 10 air samples collected during a constant altitude leg of mission 15, was 3% or 3 pptv (whichever was larger) for the alkanes and ethyne and 5% or 5 pptv (whichever is larger) for the olefins. Measurement precision for CFC-12, CFC-11, CFC-113, CH_3CCl_3, CCl_4, and C_2Cl_4 was 0.7%, 0.8%, 1.4%, 3.8%, 1.7%, and 4.2%, respectively. The precision estimates represent upper limit values because these successive samples may not have had identical mixing ratios. The limit of detection for benzene and toluene was 5 pptv, while that for the remaining NMHCs was 3 pptv. The reported halocarbons were always present at concentrations well above their detection limits.

Results

The flight paths and locations of the 1667 whole air samples collected onboard the DC-8 during missions 4 to 21 (missions 1 to 3 were test flights) are displayed in Figure 1. Figure 2 shows the grab-sampling distribution as a function of altitude and latitude and altitude and longitude. The figures reflect the good altitudinal, latitudinal, and longitudinal sampling coverage by the DC-8 but also show that in accord with the major goal of the Pacific Exploratory Mission-West the most densely sampled region was concentrated in the western Pacific between 12° and 32°N latitude and between 120° and 150° E longitude.

While attempts were made to sample many different types of air masses, the atmosphere was not randomly sampled so may bias the air mass descriptions discussed below. In addition, the very complex and diverse meteorological conditions encountered during the 6-week sampling period mean that the averaged data should not be construed to represent a particular outflow scenario. Rather, they are intended to present an averaged trace gas

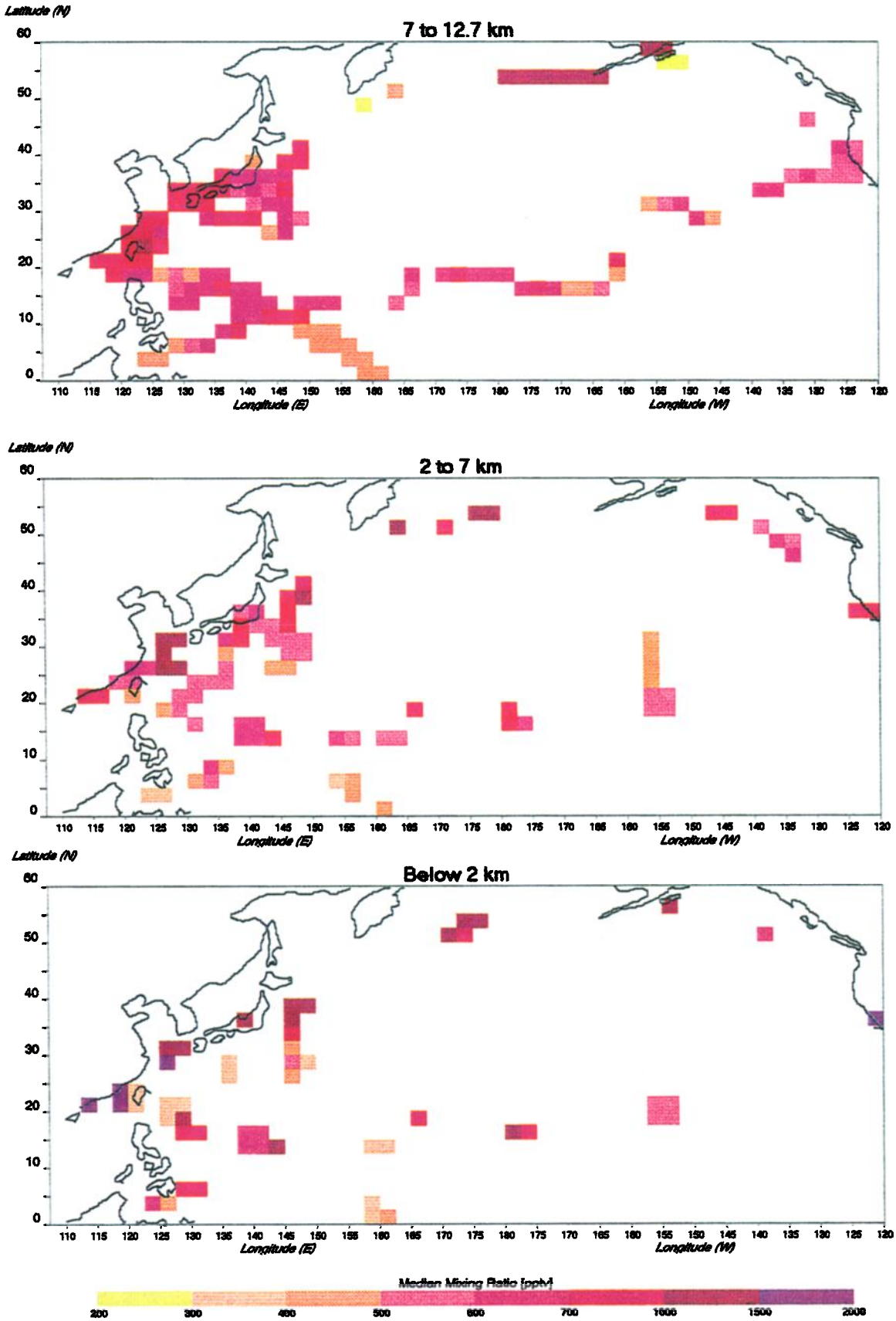

Plate 1. Ethane color patch plot for three altitude ranges.

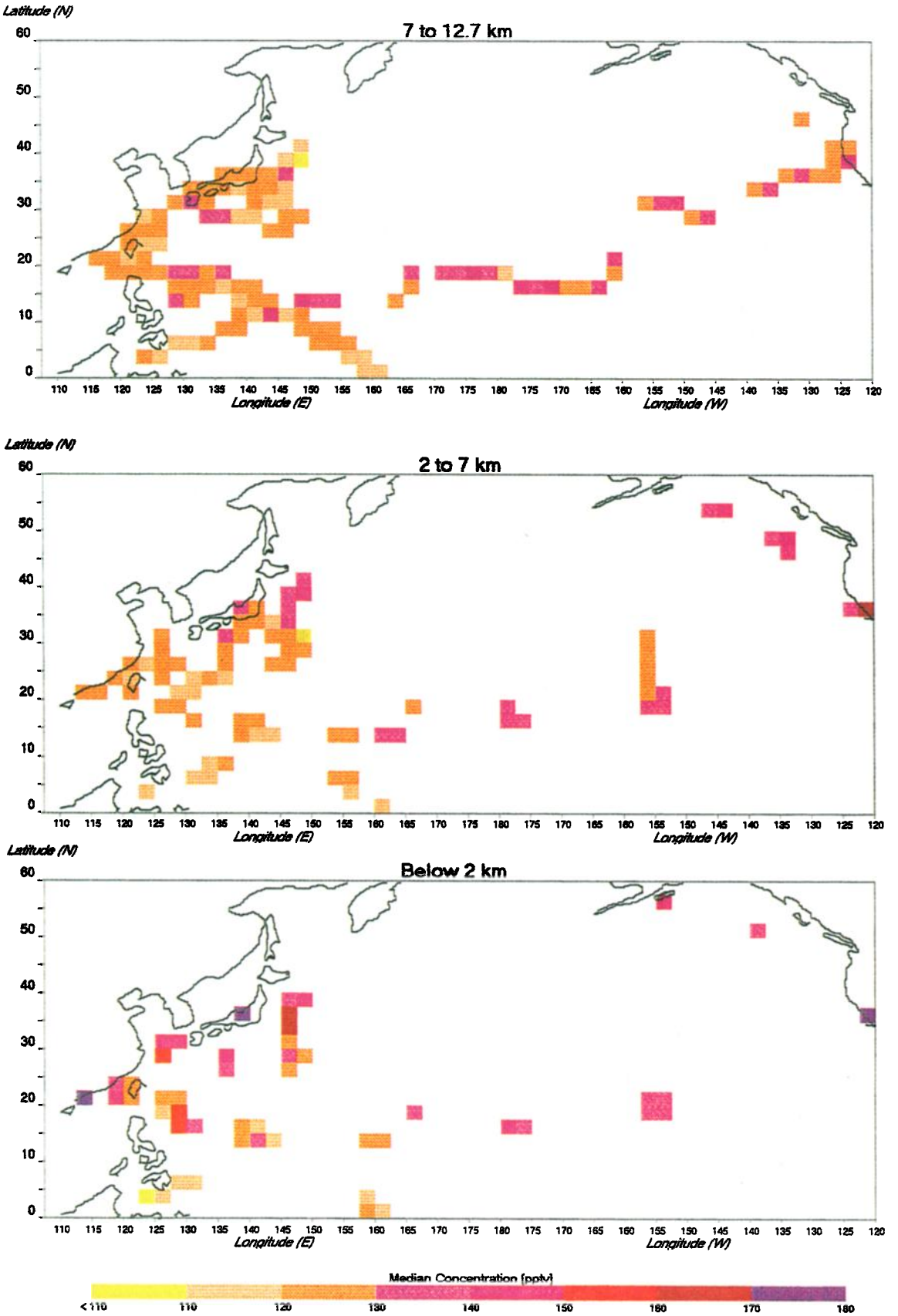

Plate 2. CH_3CCl_3 color patch plot for three altitude ranges.

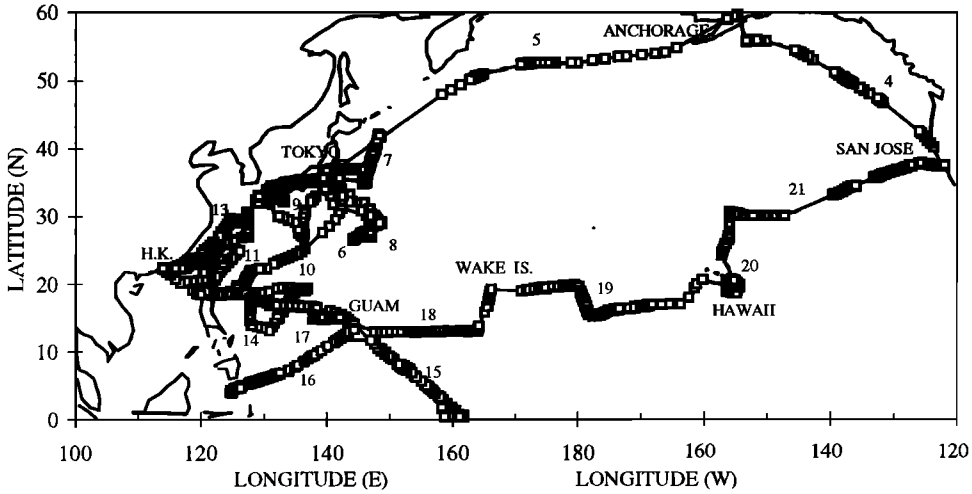

Figure 1. PEM-West A flight track and sample locations of Missions 4 to 21, with the mission number for each nearby.

distribution for the sampled areas of the northern Pacific region during September and October 1991. By contrast, the week-long intensive missions flown out of Japan, Hong Kong, and Guam allow the regional data to be considered more as a "snapshot."

The meteorological aspects of the project are described in an overview by *Bachmeier et al.* [this issue], but some general features are summarized here. The mean flows averaged for the PEM-West A time frame include a high-pressure system over the western North Pacific which, at lower tropospheric altitudes, brought marine air from the east across the Guam region and toward Japan from the south to southwest. High pressure at lower altitudes over central and eastern China tended to bring continental air across the Sea of Japan and over the East China and South China Seas. The middle and upper troposphere north of 25°-30°N was dominated by westerly flow off the Asian continent. Long-range transport was also affected by the several tropical cyclones that occurred during the mission which tended to track northeastward close to the east coast of Asia.

Fingerprint Characterization

Samples collected near large accessible NMHC and halocarbon sources such as Tokyo, Hong Kong, and San Jose and in more remote regions exhibiting enhanced mixing ratios were characterized or "fingerprinted," as was incomplete combustion from vehicle exhaust [*Blake and Rowland*, 1995]. This fingerprinting was achieved by subtracting appropriate "background" mixing ratios from each hydrocarbon and halocarbon measurement. Ideally, air of the same composition as that which originally diluted the source material would provide the background mixing ratio values. Thus, the average mixing ratios of several samples collected in close proximity immediately prior to or after encountering a "plume" exhibiting relatively enhanced trace gas mixing ratios were usually employed. After background subtraction, these residual or "excess" concentrations were added together according to their classification as NMHC or halocarbon, then the percentage contribution made to the category

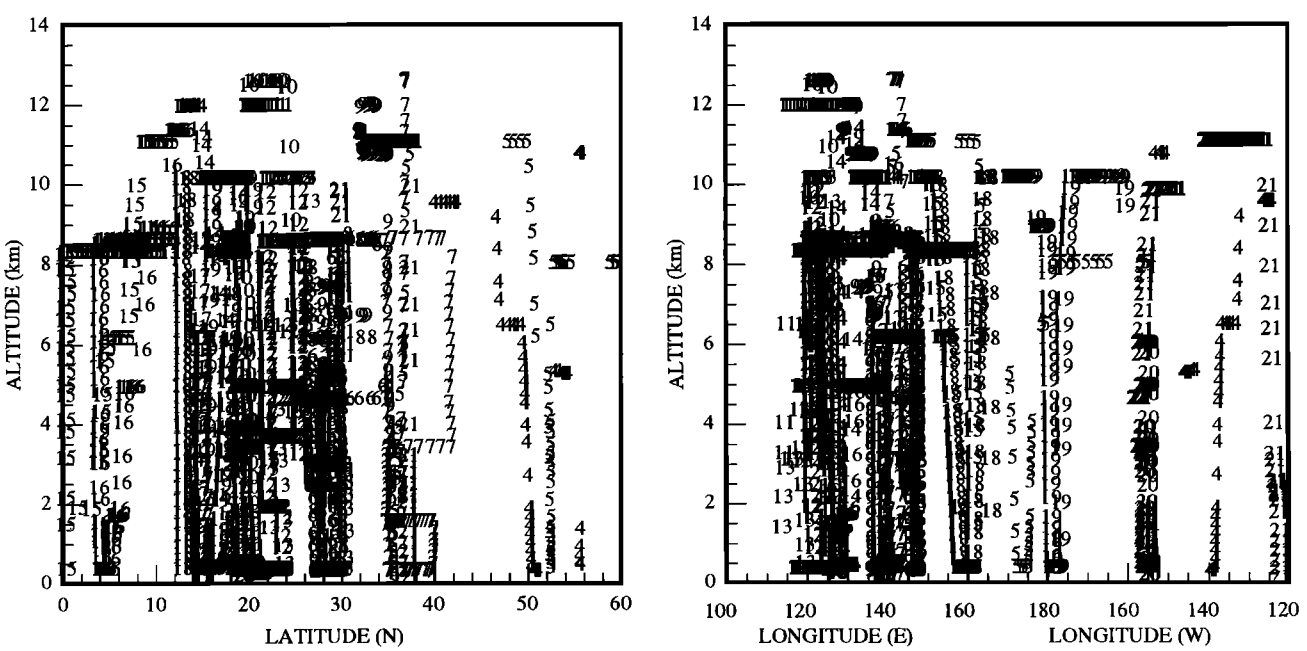

Figure 2. Sample distribution as a function of altitude between 0 and 13 km and latitude between 0° and 60°N, and as altitude and longitude between 115°E and 120°W, respectively. Each sample is designated by its corresponding mission number.

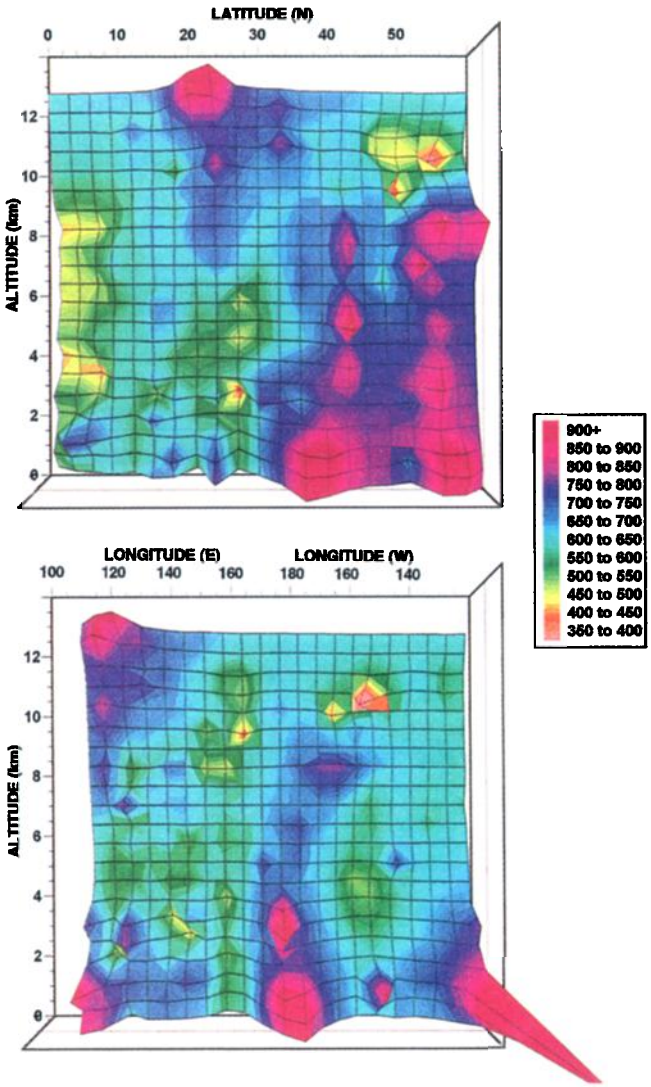

Plate 3. Ethane mixing ratios in pptv as latitude-altitude and longitude-altitude 3-D contours.

total by each trace gas was calculated. The fingerprint for a particular source was then established by averaging the percentage contributions of all samples collected near that source. Tables 1a and 1b show the background values used for each set of source samples, the excess concentrations in parts per trillion by volume (pptv), and the average percentage contributions for each source type. As an example of the fingerprint calculation, samples collected over Tokyo at the end of mission 5 contained a total halocarbon excess of 648 pptv. The excess of CH_3CCl_3 over background was 366 pptv. Thus CH_3CCl_3 represented 57% of total excess halocarbons measured in Tokyo air. Methyl chloroform was also found to be the dominant halocarbon emission from both Hong Kong and San Jose, accounting for 34% and 43% of the halocarbon total over background, respectively. This suggests that CH_3CCl_3 is likely to be an excellent tracer for polluted air parcels originating from industrial cities around the Pacific region. However, these results should be interpreted with caution as each city fingerprint was calculated employing samples collected on single aircraft approaches, and as such should serve as a guide rather than as being representative of the typical average. For example, on the approach to San Jose (October 22, 1991) a very large brush/suburban fire was taking place in the Oakland area. In addition, no samples were available from cities deep in the continent of Asia.

Table 1b shows that incomplete combustion, mainly from vehicle exhaust, is characterized by high alkene and ethyne, and low ethane and propane contributions. Table 2 shows that the alkenes are relatively short-lived in the atmosphere ($t < 2$ days) and so are expected to persist only long enough to be observed close to their source regions or as indicators of rapid air mass transport. However, ethyne has a relatively long lifetime of approximately 23 days (Table 2), allowing it to persist long enough in the atmosphere to act as a tracer for air masses that have been transported over long distances. Table 1b shows that Tokyo, Hong Kong, and San Jose also exhibit significant ethane and propane components, revealing the presence of additional hydrocarbon sources in cities, namely natural gas and propane gas used for cooking and heating [*Blake and Rowland*, 1995]. City emissions therefore represent the complex mix of incomplete combustion and natural gas and propane leakage, typical of an urban environment.

General Features

Tables 3a and 3b give the median, average, standard deviation, maximum, and minimum concentrations of the measured

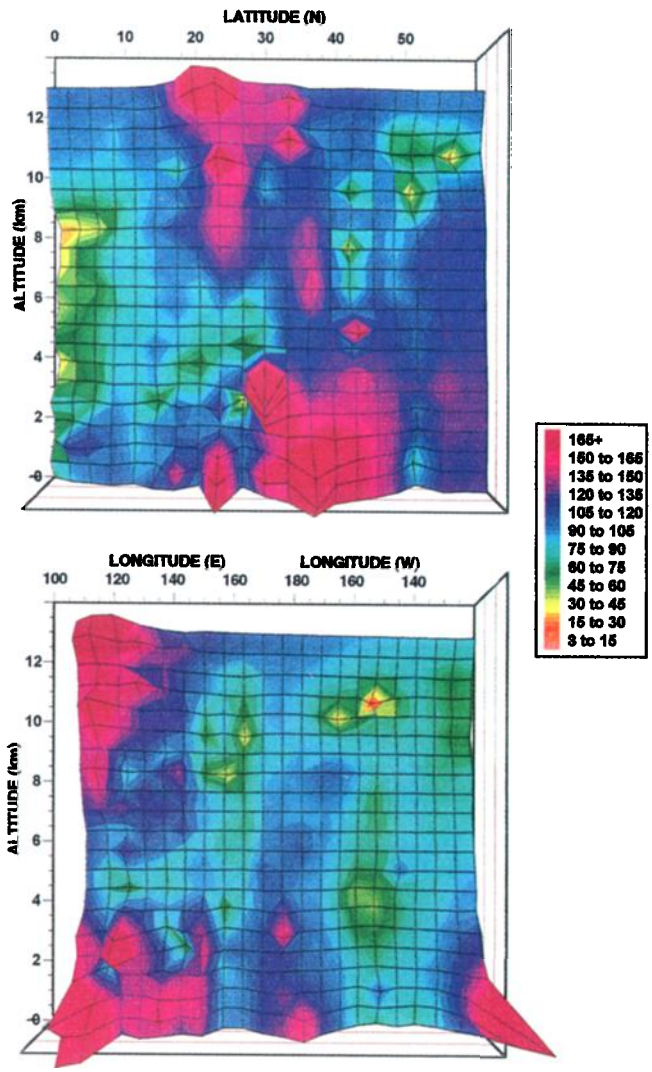

Plate 4. Ethyne mixing ratios in pptv as latitude-altitude and longitude-altitude 3-D contours.

Table 1a. Halocarbon Fingerprint Signatures From Various Urban and Individual Sources, and Selected Enhanced Plumes

	Samples	Avg Long (E)	Avg Lat (N)	Avg Alt (m)	CFC-12	CFC-11	CFC-113	CH_3CCl_3	CCl_4	C_2Cl_4
Source Fingerprints										
Tokyo, mission 5	4	139	36	530						
representative background, pptv					500	252	78	158	107	8
excess mixing ratio, pptv					75	30	82	366	19	76
fingerprint, % halocarbon contribution					12	5	13	57	3	12
Hong Kong, mission 13	1	114	22	1370						
representative background, pptv					492	258	76	137	111	5
excess mixing ratio, pptv					36	28	12	58	5	30
fingerprint, % halocarbon contribution					22	17	7	34	3	18
San Jose, mission 21	7	238	37	800						
representative background, pptv					513	267	80	162	112	13
excess mixing ratio, pptv					59	18	28	143	13	71
fingerprint, % halocarbon contribution					18	5	8	43	4	21
Incomplete combustion										
vehicle exhaust, [*Blake et al.*, 1994]										
fingerprint, % halocarbon contribution					0	0	0	0	0	0
Plume Fingerprints										
Mission 10, S Taiwan	10	124	22	12080						
average plume, pptv					502	269	78	121	111	3
representative background, pptv					502	269	78	121	111	3
excess mixing ratio, pptv					0	0	0	0	0	0
fingerprint, % halocarbon contribution										
Mission 13, S Korea	6	127	30	390						
average plume, pptv					509	271	84	159	115	16
representative background, pptv					504	263	76	117	105	5
excess mixing ratio, pptv					5	8	8	42	10	11
fingerprint, % halocarbon contribution					6	9	9	50	12	13
Mission 13, E China	13	119	23	650						
average plume, pptv					508	268	79	139	115	11
representative background, pptv					497	262	75	123	107	3
excess mixing ratio, pptv					11	5	4	15	8	8
fingerprint, % halocarbon contribution					21	10	8	30	15	16
Mission 14, S Japan	17	129	17	920						
average plume, pptv					509	268	82	146	114	11
representative background, pptv					503	267	78	122	109	4
excess mixing ratio, pptv					5	2	4	24	5	7
fingerprint, % halocarbon contribution					11	4	10	51	10	15

Table 1b. Nonmethane Hydrocarbon Fingerprint Signatures From Various Urban and Individual Sources, and Selected Enhanced Plumes

	Ethane	Ethene	Ethyne	Propane	Propene	i-Butane	n-Butane	1-Butene	i-Pentane	n-Pentane	1-Pentene	n-Hexane	Benzene	Toluene
Source Fingerprints														
Tokyo, mission 5														
representative background, pptv	676	38	112	92	0	35	53	0	25	19	0	9	45	32
excess mixing ratio, pptv	815	1153	605	892	272	517	943	71	473	298	19	211	152	1063
fingerprint, % NMHC contribution	11	15	8	12	4	7	13	1	6	4	0	3	2	14
Hong Kong, mission 13														
representative background, pptv	1038	23	311	102	8	8	18	5	6	4	0	0	65	10
excess mixing ratio, pptv	1271	667	1480	723	38	313	521	13	287	177	5	119	499	870
fingerprint, % NMHC contribution	18	10	21	10	1	4	7	0	4	3	0	2	7	12
San Jose, mission 21														
representative background, pptv	844	12	153	224	8	26	45	4	19	10	0	0	61	0
excess mixing ratio, pptv	2075	467	759	1399	151	387	756	38	550	220	44	60	146	245
fingerprint, % NMHC contribution	28	6	10	19	2	5	10	1	7	3	1	1	2	3
Incomplete combustion														
vehicle exhaust, [*Blake et al.*, 1995]														
fingerprint, % NMHC contribution	3	24	19	1	9	1	7	1	3	8	2	2	11	8
Plume Fingerprints														
Mission 10, S Taiwan														
average plume mixing ratio, pptv	1015	30	213	129	11	13	26	2	7	0	0	0	60	0
representative background, pptv	418	7	35	11	0	0	0	0	0	0	0	0	6	0
excess mixing ratio, pptv	664	20	211	125	11	13	26	2	7	7	0	0	56	0
fingerprint, % NMHC contribution	58	2	18	11	1	1	2	0	1	1	0	0	5	0
Mission 13, S Korea														
average plume mixing ratio, pptv	1641	67	436	932	15	193	391	9	125	122	0	30	112	93
representative background, pptv	1029	33	360	191	10	35	51	4	20	13	0	3	95	13
excess mixing ratio, pptv	622	41	74	695	2	145	293	5	94	98	0	27	29	80
fingerprint, % NMHC contribution	28	2	3	32	0	7	13	0	4	4	0	1	1	4
Mission 13, E China														
average plume mixing ratio, pptv	1656	110	664	514	10	103	160	7	63	42	1	12	177	42
representative background, pptv	508	19	60	47	15	2	12	7	2	3	1	0	16	5
excess mixing ratio, pptv	1148	91	603	467	-6	102	148	0	61	39	0	12	162	37
fingerprint, % NMHC contribution	40	3	21	16	0	4	5	0	2	1	0	0	6	1
Mission 14, S Japan														
average plume mixing ratio, pptv	953	41	258	228	22	48	70	9	26	19	1	5	88	24
representative background, pptv	558	48	96	43	29	6	11	15	4	3	0	3	27	18
excess mixing ratio, pptv	395	-7	162	185	-7	43	59	-5	22	16	1	3	61	6
fingerprint, % NMHC contribution	42	-1	17	20	-1	5	6	-1	2	2	0	0	7	1

Table 2. Estimated Atmospheric Lifetimes of Selected Nonmethane Hydrocarbons (NMHCs) and Halocarbons

	OH Rate [a]	Lifetime (Days) [b]
CFC-11		42-66 yr [c]
CH_3CCl_3	0.01	5.7 yr
C_2Cl_4	0.17	122
Ethane	0.27	78
Ethyne	0.90	23
Propane	1.15	18
Benzene	1.23	17
i-Butane	2.34	9
n-Butane	2.54	8
i-Pentane	3.90	5
n-Pentane	3.94	5
n-Hexane	5.61	4
Toluene	5.96	3
Ethene	8.52	2
Propene	26.3	0.8
1-Butene	31.4	0.7
1-Pentene	31.4	0.7
Isoprene	101	0.2

Rate constants for CH_3CCl_3 and C_2Cl_4 taken from *DeMore et al.* [1992].

Rate constants for NMHCs taken from *Atkinson* [1990].

[a] Units, 10^{-12} x k(298).

[b] Lifetimes of hydrocarbons are calculated by comparison with the CH_3CCl_3 lifetime of 5.7 years, *Prinn*, [1992].

[c] *WMO*, [1992].

hydrocarbons and halocarbons after the data have been separated into three altitude sections, 7 to 12.7 km, 2 to 7 km, and below 2 km, which were chosen to represent the middle-upper free troposphere, lower free troposphere, and planetary boundary layer (PBL), respectively. There are 533, 713, and 421 air samples in each section, which constitute approximately 21%, 38%, and 22% of the total air column, respectively [U.S. Standard Atmosphere, 1976]. All compounds exhibit higher mixing ratios in the PBL due to the proximity of surface sources. However, the NMHCs (Table 3b) typically show higher median concentrations in the middle-upper and PBL altitude sections than in the lower free troposphere. This was a general feature of the NMHCs and will be discussed in more detail below. Several of the very short lived hydrocarbons ($t < 1$ day, see Table 2), including 1-pentene and isoprene, were below their detection limits in all samples except for those collected in the PBL very close to their continental sources.

Color patch plots showing the latitudinal and longitudinal variation of the concentrations of ethane and methyl chloroform are given in Plates 1 and 2, respectively. They show the spatial variation of the median trace gas mixing ratios for a latitude-longitude grid size of 2.5° by 2.5°. As expected, the highest concentrations of both ethane and CH_3CCl_3 were observed at low altitude close to the continental sources such as San Jose, California (37.3°N, 121.9°W); Anchorage, Alaska (61.2°N, 149.9°W); Tokyo, Japan (35.7°N, 139.75°E); Hong Kong (22.3°N, 114.2°E); and Guam (13.7°N, 145.0°E). Honolulu, Hawaii (21.3°N, 157.9°W), was not a "hot spot" because mission 20 had been designed specifically to study downdrafting over the Island of Hawaii, and no samples were taken in the vicinity of Honolulu. Elevated ethane concentrations were also observed in the free troposphere near the western Pacific coast and over Guam.

The lower free tropospheric sections of Plates 1 and 2 display similar features to the PBL region throughout the longitude and latitude range covered. However, in the PBL the mixing ratios of ethane (Plate 1) range from 300 to 2000 pptv and from 300 to 1500 pptv in the lower free troposphere, where smaller absolute values were observed for all hydrocarbons and halocarbons. In the middle-upper troposphere ethane ranges from 200 to 1250 pptv, indicating that the direct effect of urban centers is still less

Table 3a. Median, Average, Standard Deviation, Maximum, and Minimum Halocarbon Observations During PEM-West A

	CFC-12	CFC-11	CFC-113	CH_3CCl_3	CCl_4	C_2Cl_4
7 - 12.7 km N=533						
Median	508	274	87.9	155	121	3.0
Average	508	274	87.7	154	120	3.3
S.D.	5	5	3.0	13	5	1.7
Minimum	492	243	68.6	86	94	0.1
Maximum	520	297	111.5	205	168	25.0
2 - 7 km N=713						
Median	509	274	88.1	155	121	3.2
Average	509	273	88.0	156	121	3.9
S.D.	7	5	2.4	14	3	2.5
Minimum	479	250	79.5	122	108	0.1
Maximum	545	295	98.3	232	131	16.8
< 2 km N=421						
Median	509	274	89.0	162	122	4.6
Average	512	274	92.5	176	122	9.0
S.D.	19	8	24.1	75	5	21.1
Minimum	487	252	77.8	126	96	0.9
Maximum	696	342	464.4	994	166	250.3

N, number of samples analyzed at each altitude range.

apparent. However, consistent with the high median middle-upper tropospheric ethane mixing ratios shown in Table 3, the general spread of continental influence is more extensive than in the lower free troposphere.

Altitudinal mixing ratio distributions calculated over the PEM-West A latitude and longitude range are described in Plates 3 to 10 for selected NMHCs (ethane, ethyne, propane, benzene, and i-pentane) and halocarbons (CH_3CCl_3, C_2Cl_4, and F-11) as three-dimensional color contour plots based on 3° by 635 m and 6.3° by 635 m latitude-altitude and longitude-altitude grids, respectively. Interpolation of the data between grid squares is achieved employing an inverse-distance weighting algorithm. These figures have much better vertical resolution than the patch plots (Plates 1 and 2) and show clearly the variable vertical extent of the influence of surface sources and trends of the different-lived gases. They provide a useful perspective for characterizing the regional large scale trace gas distribution and transport encountered during PEM-West A. However, as was stated earlier, the atmospheric sampling was neither random nor uniform (see Figures 1 and 2). Therefore, Plates 3 to 10 should always be compared with the appropriate grab-sampling distribution described in Figure 2. The nonrandom nature of the sampling strategy was especially significant for the boundary layer region, where the airport landings accounted for many samples for those altitudes. As their inclusion would strongly bias the lower-altitude distribution to overrepresent urban airport locations, 18 low-altitude airport samples were removed from the 3-D contour plot database.

The NMHCs and halocarbons shown in Plates 3 to 10 were chosen to represent a wide range of different lifetimes and possible sources with which to interpret the large scale PEM-West A features. All the gases show relatively high concentrations near the urban source regions, but the longer-lived NMHCs such as ethane, ethyne, and propane (Plates 3, 4 and 5), show enhanced regions at all altitudes. Except for a high-altitude region between 10 and 12.5 km, relatively short-lived i-pentane (which has a lifetime of only about 5 days) quickly decayed to levels below its detection limit (Plate 7). In accord with their very long lifetimes and high background concentrations, the long-lived halocarbons, CH_3CCl_3 and F-11 (Plates 8 and 10, respectively) show little mixing ratio variability away from the source regions.

A feature of both the patch and the 3-D contour plots (Plates 1 to 10) is the latitudinal gradient of trace gases, with the lowest mixing ratios occurring around the equator, and increasing with latitude. The highest levels are usually above 30°N. This reflects both the proximity of continental sources at higher latitudes and the large-scale airflow regime, which featured strong continental outflow north of about 25°N in the midtroposphere and about 30°N in the upper troposphere [*Bachmeier et al.*, this issue]. In addition, the mean cold frontal position near the Asian continent was between 20° and 40°N [*Bachmeier et al.*, this issue]. The latitudinal trend for ethane (Plates 1 and 3) is more pronounced in the planetary boundary layer and the lower free troposphere than in the middle-upper free troposphere. This gradient was sharpened by the very clean air that was swept north to the Guam region by Typhoon Pat (mission 15) [*Bachmeier et al.*, this issue]. The clean equatorial air to the south is also well described by the CH_3CCl_3 contour plot shown in Plate 8.

A longitudinal gradient is also evident, particularly for ethyne (see Plate 4) and benzene (Plate 6), where typically higher mixing ratios occur near the Asian continent, Japan, and the North American continent. Up to about 4 km (a few hundred meters

Table 3b. Median, Average, Standard Deviation, Maximum, and Minimum NMHC Observations During PEM-West A

	Ethane	Ethene	Ethyne	Propane	Propene	i-Butane	n-Butane	1-Butene	i-Pentane	n-Pentane	1-Pentene	n-Hexane	Isoprene	Benzene	Toluene
7 - 12.7 km N=533															
Median	667	14	99	48	4	<3	6	<3	<3	<3	<3	<3	<3	19	<5
Average	667	17	114	57	4	4	9	<3	<3	<3	<3	<3	<3	24	<5
S.D.	175	10	73	36	6	6	11	<3	<3	<3	<3	<3	<3	20	<5
Minimum	191	<3	<3	<3	<3	<3	<3	<3	<3	<3	<3	<3	<3	<5	<5
Maximum	1250	73	467	194	40	37	73	22	42	28	11	10	<3	168	80
2 - 7 km N=713															
Median	564	13	74	34	4	<3	4	<3	<3	<3	<3	<3	<3	19	<5
Average	621	24	103	54	11	6	11	3	3	<3	<3	<3	<3	25	6
S.D.	220	36	107	59	23	19	22	7	8	<3	<3	<3	<3	24	13
Minimum	339	<3	16	5	<3	<3	<3	<3	<3	<3	<3	<3	<3	<5	<5
Maximum	2554	370	1099	526	265	404	179	91	64	47	57	29	32	241	197
< 2 km N=421															
Median	634	25	103	44	10	6	9	4	3	4	<3	<3	<3	30	7
Average	758	82	172	150	27	40	70	8	41	24	<3	10	<3	53	49
S.D.	414	327	265	318	79	165	290	24	255	134	<3	60	<3	98	367
Minimum	302	5	16	5	<3	<3	<3	<3	<3	<3	<3	<3	<3	<5	<5
Maximum	3100	5183	3327	4237	1148	2801	4805	389	4407	2457	150	995	304	1507	7009

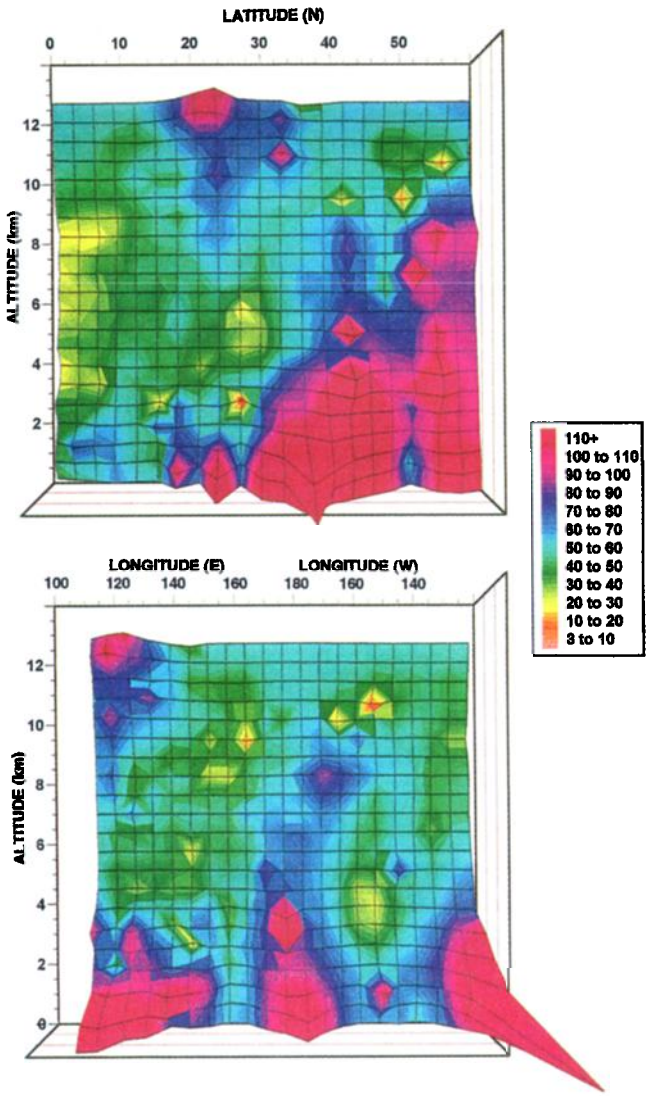

Plate 5. Propane mixing ratios in pptv as latitude-altitude and longitude-altitude 3-D contours.

above the observed boundary layer height) dome-shaped isolines are identifiable over the urban centers such as Hong Kong, Tokyo, and San Jose (e.g., Plate 9). Short-lived i-pentane (Plate 7) illustrates how the large-scale airflow transports emissions rapidly from these western Pacific source regions between 30° and 40°N up to about 3 km, followed by northeasterly advection over the Pacific.

Because of local downdrafting conditions the lower tropospheric region over the Island of Hawaii had particularly low mixing ratios for all NMHCs, comparable to the observations of background Pacific levels as shown in Plates 3 to 7. Most of the C_2Cl_4 observations over the Island of Hawaii (see Plate 9) were between 3 to 5 pptv instead of levels in the region of 10 pptv or higher encountered in other urban areas.

In addition to the direct vicinity of urban source regions, some remote PBL areas exhibited elevated mixing ratios. For example, elevated levels of ethane, CH_3CCl_3 (see Plates 1 and 2), ethyne, and propane (Plates 4 and 5), were observed around 15°N, 180°E between Hawaii and Wake Island during mission 19. Trajectory analysis suggests these urban signature gases may have originated from the Hawaiian area [*Merrill*, this issue]. Elevated levels of trace gases such as ethane (see Plate 1) were observed for all altitude sections along the Aleutians during mission 5 and near the eastern Chinese coast during mission 13, both of which have trajectories suggesting influence of Asian continental origin [*Merrill*, this issue]. Higher levels were observed near the North American and the eastern Asian coasts, with lower levels in the mid-Pacific.

Except when near urban sources, hydrocarbons such as ethane (Plate 3) have significantly more small scale structure than the much longer-lived gases such as CFC-11 (see Plate 10). This enhanced hydrocarbon structure is in addition to source locations and regional scale transport features and occurs because photochemical removal by hydroxyl is extremely important in determining the distribution of the relatively short lived NMHC species. Contributing to the relatively small scale variability in the concentrations of many of the trace gases (as seen in Plates 1-10), tropical storm Luke (mission 6) and Typhoons Mireille (mission 9) and Nat (mission 10) transported clean Pacific air north to the Japanese region. Therefore the highly structured features of the data reflect the influence of both transport and photochemistry on the complicated mix of sources and their distributions.

The ethane contours in Plate 3 show two prominent features, both at an altitude of 11 km, and exhibiting very low

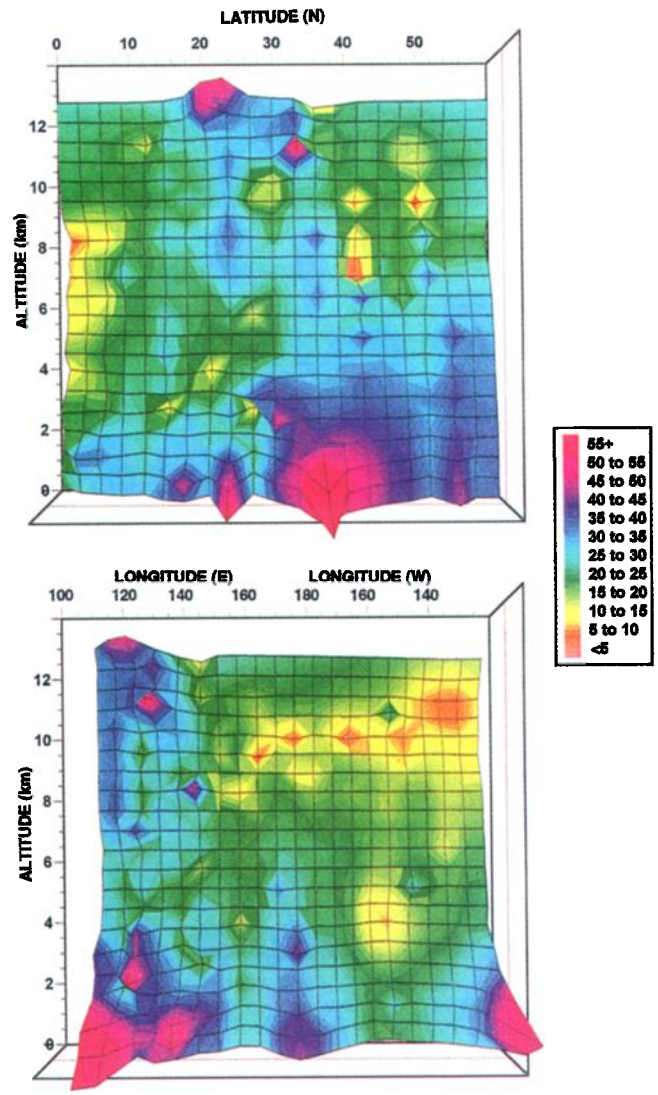

Plate 6. Benzene mixing ratios in pptv as latitude-altitude and longitude-altitude 3-D contours.

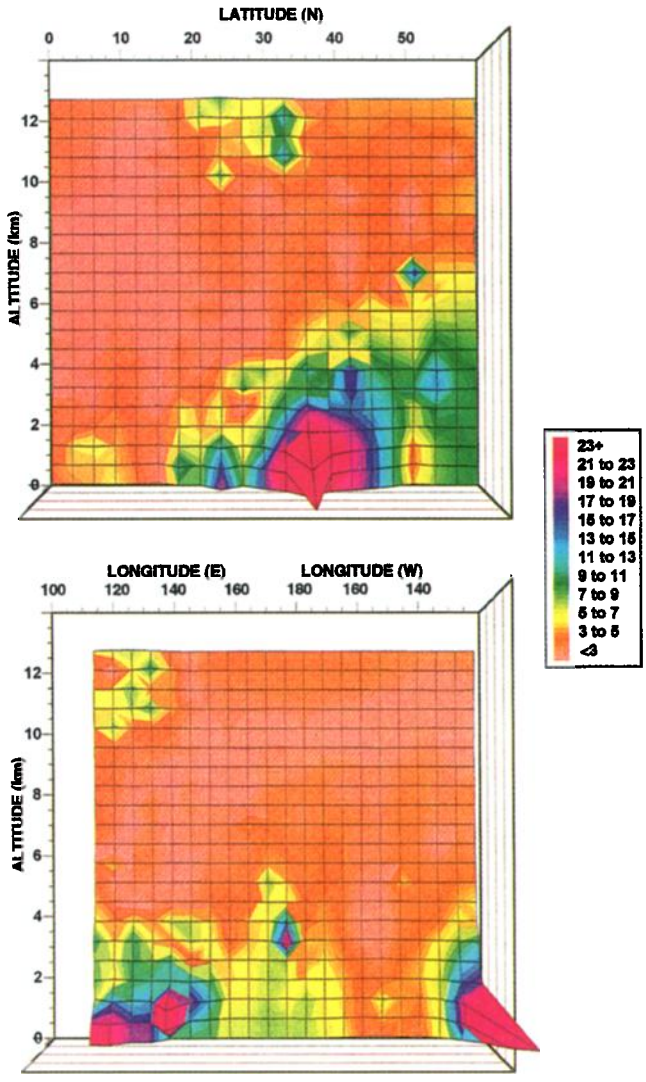

Plate 7. i-Pentane mixing ratios in pptv as latitude-altitude and longitude-altitude 3-D contours.

concentrations. They are centered at 55°N and 48°N for the altitude-latitude contour and at 155°W and 160°E for the altitude-longitude contour. These features represent samples that were collected near Anchorage, Alaska, and south of the Kamchatka Peninsula, Russia, during missions 4 and 5 (San Jose-Anchorage-Tokyo). Both regions were associated with very high ozone concentrations due to intrusions of stratospheric air [*Bachmeier et al.*, this issue]. The CH_3CCl_3 and C_2Cl_4 contour plots, shown in Plates 8 and 9, also clearly illustrate the position of the intrusion encountered near Anchorage during mission 4. However, mixing ratio data for C_2Cl_4 and CH_3CCl_3 were not available for most of mission 5 because of analytical difficulties encountered at the beginning of the field mission. These problems also meant that CFC-11 data were affected for both missions 4 and 5. In addition, water vapor levels were extremely low in the stratospherically influenced air masses of missions 4 and 5, causing wall losses to occur for some of the assayed halocarbons. Subsequently, it has been found that the addition of small aliquots of purified water vapor to each sample canister immediately prior to its deployment in the field effectively eliminates such losses.

Rapid Vertical and Long Range Transport

The previous discussions of Table 3b and Plates 1 to 7 revealed that a strong feature of the averaged PEM-West A data was a free-tropospheric mixing ratio enhancement, typically above 7 km. In addition, 13 out of the 18 missions show at least one vertical profile where the trace gas concentrations increase with altitude. Such observations are consistent with the earlier STRATOZ II and STRATOZ III campaigns which took place in the Atlantic [*Ehhalt et al.*, 1985; *Rudolph*, 1988; *Ehhalt*, 1992] and with the Atmospheric Boundary Layer Expedition (ABLE) 3A, and ABLE 3B projects in Alaska and eastern Canada [*Blake et al.*, 1992, 1994].

A typical vertical profile of ethyne up to 8 km is shown in Figure 3. This vertical ascent was made approximately 1000 km SE of Tokyo during mission 8 and exhibits enhanced ethyne mixing ratios both in the PBL and above 7 km, with relatively low concentrations at intermediate altitudes. Trajectories show that two days prior to being sampled, the air at 8 km had been transported from northern India, over central China, then southern Japan, while the cleaner lower free tropospheric air exhibited trajectories with central Pacific origins [*Merrill*, this issue]. An important tropospheric mechanism for the injection of such relatively high concentrations of trace gases into the middle and upper troposphere has been suggested previously by *Ehhalt et al.*

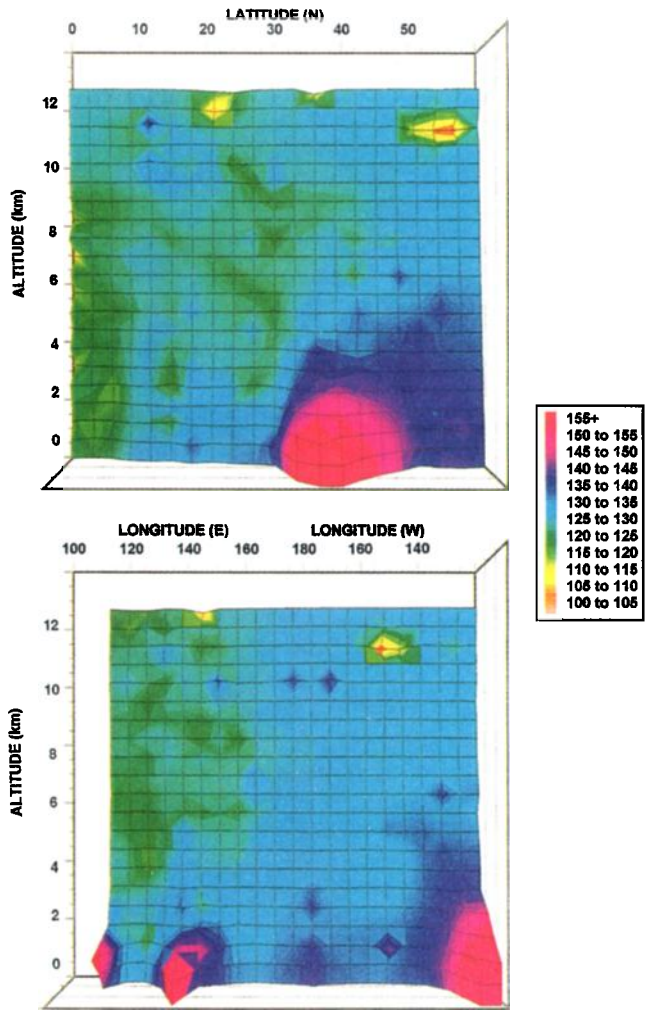

Plate 8. CH_3CCl_3 mixing ratios in pptv as latitude-altitude and longitude-altitude 3-D contours.

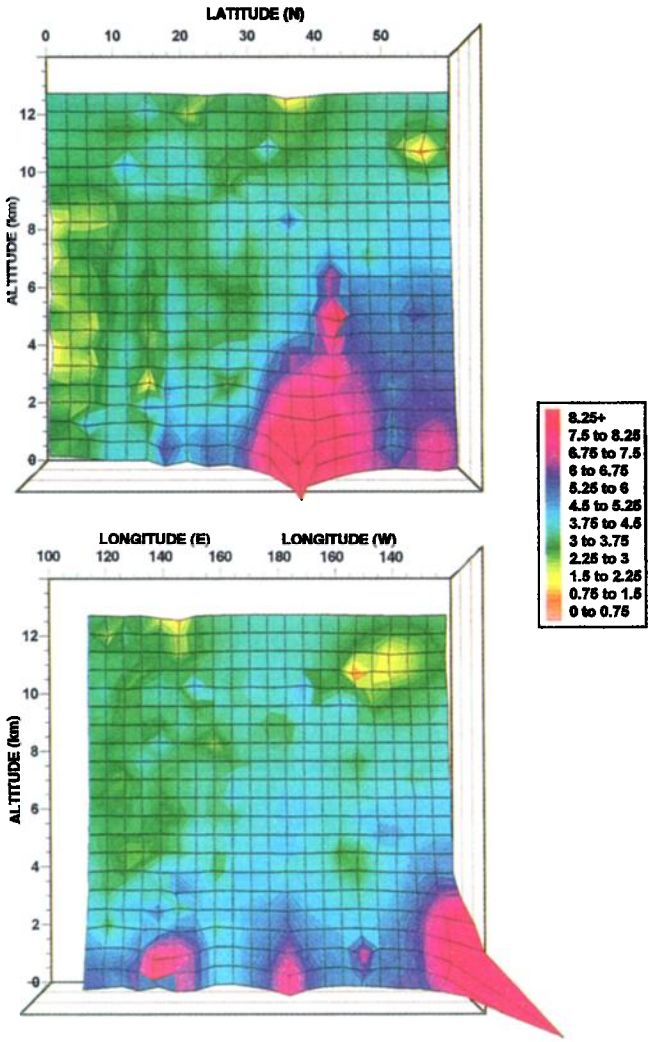

Plate 9. C_2Cl_4 mixing ratios in pptv as latitude-altitude and longitude-altitude 3-D contours.

[1985] and others to be rapid vertical transport. Vertical structure, such as that shown in Figure 3, represents the free tropospheric enhancement as a layer that is not directly coupled to a source region, implying that the trace species do not originate from immediate local sources but are more likely from convective events in the continental interior, followed by long-range transport. The generally high levels of longer-lived ethyne (see Plate 4) and low levels of very short-lived NMHCs observed in the middle-upper troposphere (see Table 2 for lifetimes) also suggest that the sources had a large combustion constituent and may originate from deep in the Asian continent. In support of this, trajectory analysis suggests that a large number of middle-upper tropospheric air parcels sampled had deep continental origins [*Merrill*, this issue]. The general trend of relatively high mixing ratios of ^{210}Pb (a good tracer for continental air) observed up to 10 km near the Asian continent also supports an Asian continental origin for much of the trace gas enhancement observed over the western Pacific at all altitudes [*Talbot et al.*, this issue].

A related feature, seen in many of the latitude-altitude hydrocarbon contour plots, particularly ethane (see Plate 3), is a region of high concentration centered at about 56°N and 8 km that was sampled over the Aleutian Islands during mission 5. Because few samples were collected above and below 8 km at this latitude (see Figure 2) the feature appears to be decoupled from the sources below. Also, Plate 3 includes samples from mission 4 which were collected only a few degrees south of the enhanced mission 5 samples, but were separated by more than 40° in longitude from those from mission 5, and which have lower mixing ratios. The difference between the two missions is illustrated in Figure 4 which shows two vertical profiles of ethane. One profile, showing significantly lower ethane mixing ratios at all altitudes (0-8 km), was made during mission 4 in the Gulf of Alaska (46.8°-51.1°N and 131.7°-139.4°W), the other took place during mission 5 along the Aleutian Islands (52.6°N and 177.7°W-175.1°E). Thus the mission 5 enhancement is likely to have been a more general free tropospheric feature than it appears in the latitude-altitude plot of Plate 3, demonstrating the importance of using Figure 2 and both latitude and longitude 3-D contour plots in conjunction.

The air mass exhibiting the general enhancements observed during mission 5 has a back trajectory originating from the region of northeastern Siberia and Kamchatka [*Merrill*, this issue]. It also exhibits particularly high concentrations of methane [*Collins et al.*, this issue], ethane, and propane. This composition suggests a source resembling natural gas and/or venting from oil fields. However, the lack of halocarbon data for those samples makes the source determination less certain. In addition to natural gas, it

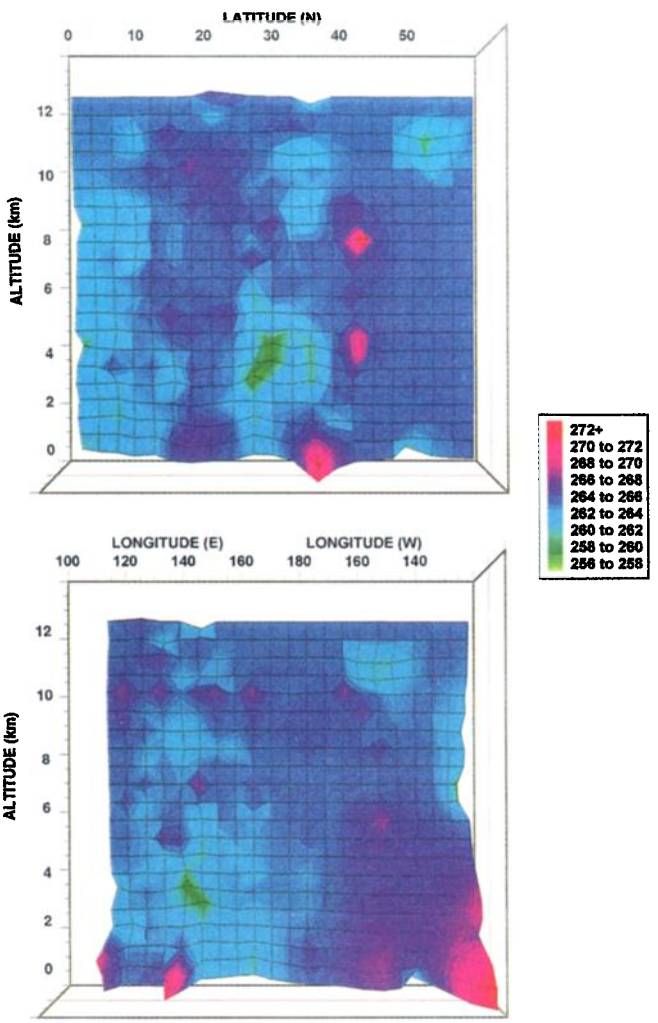

Plate 10. CFC-11 mixing ratios in pptv as latitude-altitude and longitude-altitude 3-D contours.

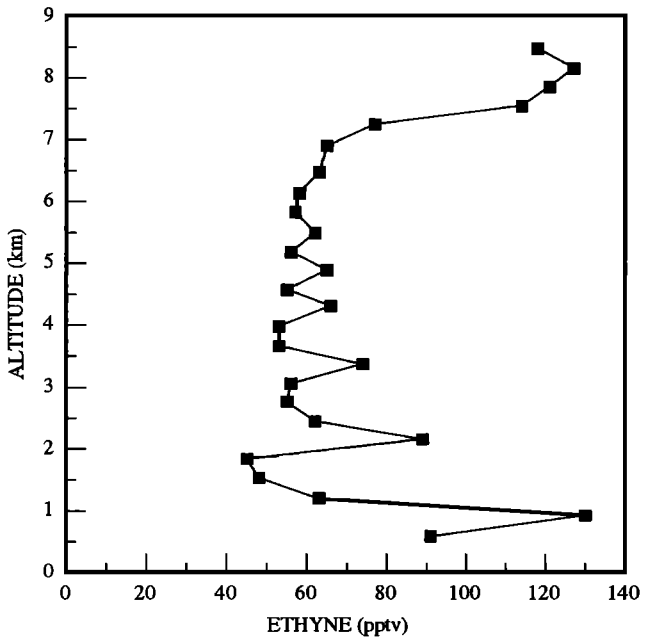

Figure 3. Typical vertical profile of ethyne in pptv made over the Pacific SE of Japan during Mission 8.

is possible that this air mass could have originated in the region of Siberia, then spent days to weeks over the Bering Sea. At that point most of the reactive NMHCs would have been photochemically oxidized by HO, leaving the observed signature of enhanced long-lived hydrocarbons.

The potential for a typhoon to drive rapid vertical transport is illustrated for NMHCs as a large hydrocarbon-enhanced plume centered at about 22°N and 120°E over the Pacific at 12.5 km and shown for ethane, ethyne, propane, and benzene in Plates 3 to 6, respectively. This air mass was sampled at the end of mission 10 east of Taiwan and southwest of Okinawa (19.0° to 24.0°N and 120.9° to 125.7°E). Ten samples were collected in the plume and their halocarbon and hydrocarbon concentrations are shown in Tables 1a and 1b, respectively. It can be seen that methane, ethane, ethyne, propane and other nonmethane hydrocarbons were significantly enhanced above the very low concentrations associated with the air surrounding it. However, the halocarbon and hydrocarbon composition of this high-altitude plume are very similar to the background boundary layer levels employed for the Hong Kong (mission 13) and South Korea (mission 13) plumes (Tables 1a and 1b). The halocarbon concentrations associated with this plume were not enhanced and confirmed that the air mass sampled in mission 10 had not come directly from a heavily industrialized urban source area such as Tokyo or Hong Kong. This is consistent with meteorological analysis which suggests that fast convection associated with nearby Typhoon Nat, was likely to have swept surface air up to the upper troposphere [*Bachmeier et al.*, this issue]. Thus the aged free tropospheric air at high altitude probably had a very different origin from this plume, precluding its use to represent appropriate plume background conditions.

Further evidence of typhoon activity affecting the high-altitude atmospheric trace gas composition was observed during mission 9 and can be located on the NMHC contour plots (Plates 3 to 7) as two enhanced regions between 10 and 12.5 km, centered at approximately 33 °N and 130°E. The entire high-altitude portion of this mission, which took place along the perimeters of Kyushu and Shikoku, the southernmost of the four main Japanese islands (32.0°-35.2°N, 129.1°-137.0°E), exhibited enhanced NMHC mixing ratios. Transport of these gases above 10 km is attributed to the fast convective transport observed near the top of Typhoon Mireille [*Newell et al.*, this issue] which, during mission 9, was centered approximately 50 km to the southwest of Nagasaki, Kyushu Island, Japan (32.2°N, 129.0°E). Plate 7 shows that the short-lived NMHC i-pentane (lifetime about 5 days) exhibited a greater enhancement than for the mission 10 plume, which was sampled in the same altitude range approximately 10° to the south. Dimethyl sulfide, which is a useful marker for oceanic boundary layer air, was also elevated above the free tropospheric background levels [*Newell , et al.* this issue]. The presence of these gases suggests that the air in this mission 10 plume was more recently in contact with the surface. The ethane enhancement seen in Figure 5 for mission 9 is relatively small in comparison to that for mission 10 and the halocarbons were not significantly enhanced; however, the NMHC concentrations indicate the influence of some combustion from the western Pacific coastal regions.

Small Scale Features

Two plumes of interest were encountered during mission 13. In the first plume, six samples were collected at 390 m altitude about 300 km off the eastern Chinese coast. Trajectory analysis indicates the air parcel came from South Korea the previous day [*Merrill* , this issue]. The fingerprint is shown in Tables 1a and 1b (South Korea). The second plume encounter was at 650 m over the Taiwan Strait (between China and Taiwan) during which 13 samples were collected (see eastern China plume in Tables 1a and 1b). This air parcel had been moving south along the eastern Chinese coast for the previous 5 days [*Merrill,* this issue]. Both plumes had enhanced CH_3CCl_3, and C_2Cl_4 concentrations and low concentrations of short-lived alkenes compared to the alkanes and ethyne, indicating that they were urban in origin but had undergone photochemical aging for at least 2 days. The eastern China plume had propane, n-butane, and ethyne contributions

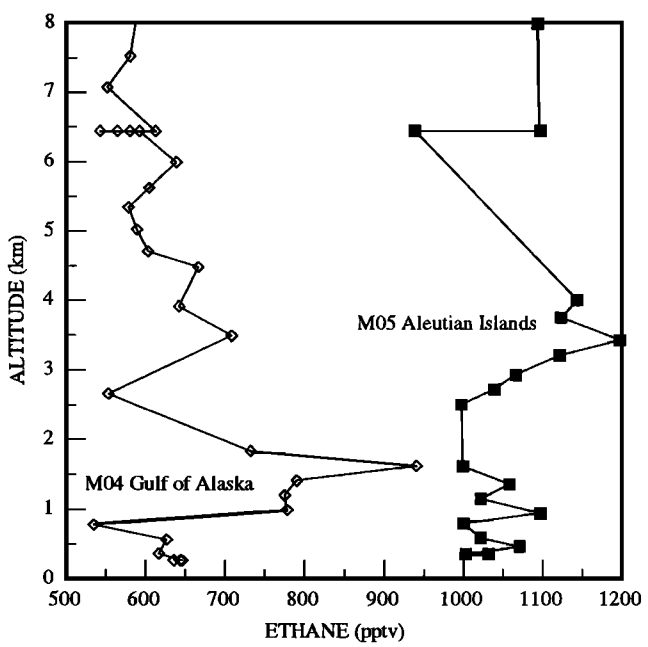

Figure 4. Vertical profiles of ethane in pptv made over the Gulf of Alaska during Mission 4 and near the Aleutian Islands during Mission 5.

more similar to those of Tokyo than Hong Kong. By contrast, the South Korea plume had lower ethyne and the highest propane contribution, which may indicate greater use of bottled propane for cooking and/or heating in its region of origin. However, further characterization of these two NMHC fingerprints is very difficult in the absence of source data from Korea and China.

If the two mission 13 halocarbon fingerprints are compared with those for Tokyo and Hong Kong, it can be seen that CH_3CCl_3 is the dominant halocarbon species, accounting for 50% of total halocarbons over background in the first South Korea plume and 30% in the second eastern China plume. However, the CCl_4 contribution of 3% to the Tokyo and Hong Kong fingerprints is very small, whereas the CCl_4 contribution from the South Korea and eastern China plumes was much higher at 12% and 15%, respectively. With the exception of CCl_4, the eastern China halocarbon fingerprint was very similar to that for Hong Kong, and the South Korea halocarbon fingerprint was more similar to that of Tokyo, probably due to the different types of industry and consumption in each region of origin.

Another plume, encountered during mission 14 at an altitude of 430 m and at a location about 500 km northeast of the Philippines, was quite different in character. As shown in Table 1a, the halocarbon fingerprint, calculated from 17 plume and 2 background samples, was, except for C_2Cl_4, almost identical to that of Tokyo. Methyl chloroform was again the dominant halocarbon constituent. Trajectory analysis shows that the air parcel traveled over southern Japan and had recently been in close proximity to South Korea [*Merrill*, this issue]. The NMHC fingerprint in Table 1b shows that the percentage NMHC composition follows the order of atmospheric lifetime for each NMHC (Table 2), with the alkenes and shorter-lived alkanes having decayed to or near zero concentrations over background, suggesting that the air parcel had undergone substantial photochemical removal and dilution with pristine background air. This is a likely scenario because the encounter took place on the western outskirts of Typhoon Orchid. Thus, the air parcel had probably spent 2 to 3 days over the Pacific Ocean prior to being sampled [*Merrill*, this issue].

Comparison With Previous Work

Several sets of vertical profiles have been published describing trace gas measurements over the Atlantic and elsewhere over the Pacific Ocean [*Ehhalt et al.*, 1985; *Dickerson et al.*, 1987; *Rudolph*, 1988; *Singh et al.*, 1988; *Greenberg et al.*, 1990; *Bonsang et al.*, 1991; *Blake et al.*, 1992; *Ehhalt*, 1992], with four sets from the Pacific regions of northern California, Alaska, and French Polynesia. The PEM-West A project provided an opportunity to cover a large part of the northern and western Pacific, collecting the largest number of whole air samples in this region of any project to date. No hydrocarbon vertical profiles were previously available for the western Pacific region. The STRATOZ II and STRATOZ III results were published in the form of latitude-altitude profiles [*Ehhalt et al.*, 1985; *Rudolph*, 1988] and took place in April - May 1980 and June 1984 over the Atlantic. *Singh et al.* [1988] provides a NMHC vertical profile over northern California (38°N) for February 1985, and *Bonsang et al.* [1991] have published NMHC profiles over the Hao atoll (18.1°S, 141.0°W) for May to June 1987. Vertical profiles over Bristol Bay, Alaska (61.1°N, 162.0°W) and the Bering Sea (58.3°N, 168.0°W) during ABLE-3A in August, 1988 were published by Blake et al. [1992].

Using data from STRATOZ and other missions, *Hough* [1991] developed a latitudinally averaged two-dimensional model. Comparison of the PEM-West A contours to Hough's model prediction for July and October indicates that the PEM-West A ethane measurements exhibited lower surface values between 30°N and 60°N. Ethane levels were in the range of 400 - 600 pptv compared to the 750 to 1250 pptv predicted by Hough's model. Perhaps the lower values were a result the PEM-West A flight tracks being further away from the continent compared to STRATOZ II and III which were flown in the Atlantic. Convective activity over the equatorial region is suggested by the PEM-West A contours. Convection associated with elevated NMHCs over the equatorial Pacific was encountered in February 1992 during the AASE II project (D. R. Blake et al., unpublished data, 1995). In addition to the lower ethane concentrations and lack of polluted equatorial convection, the observed typhoon-driven convection to the upper troposphere was not addressed by Hough's model. During PEM-West A the propane concentrations in the equatorial and subtropical regions were 50 pptv or less, while the model predicts levels of up to 250 pptv near the equatorial surface, decreasing to 50 pptv at 12 km. However, the model successfully predicts the observed enhancement in the middle-upper troposphere at latitudes above 40°N. The PEM-West A results compliment the existing data and should add significantly to the development and refinement of models.

Conclusions

The results presented here cover a suite of trace gases with lifetimes ranging from approximately 50 years to as short as a few hours (see Table 2), providing a valuable tool with which to study transport processes and the impact of Asian pollutants on the Pacific region. Data from the PEM-West A mission appear to confirm that the occurrence of enhanced mixing ratios of NMHC and other trace gases in the middle-upper free troposphere is caused by convective processes, including convective outflow from the Asian continent. Cloud-driven convective activity over land and typhoon-driven convection over the ocean strongly influenced the distribution of trace gases over the northern Pacific. The collection of urban samples has established CH_3CCl_3 as a good tracer for coastal Asian industrial activity. This study also underlined the need to identify and characterize different pollution sources in Asia. This project established a three-dimensional distribution for a large suite of trace gases in a season with expected minimum continental outflow and set a good foundation for comparison with the maximum continental outflow events expected during the PEM-West B project flown in early 1994.

Acknowledgments. The authors thank the following research group members for their assistance in the fabrication of the experimental apparatus and support during the field mission: K. Camer, B. Chisholm, R. Iyer, M. McEachern, T. Merrill, A. Potts, P. Russell, M. Schaeffer, M. Sergeant, B. Sive, and in addition, S. Sudo from the University of Tokyo. The authors especially thank D. H. Ehhalt for manuscript suggestions during the early stages of this paper. We are again indebted to Ralph Kolbush, director of the UCI Machine shop. The opportunistic filling of air canisters when an interesting atmospheric air parcel was encountered by the DC-8 was dependent upon the timely relay of information from the operators of real-time, onboard instrumentation. We especially thank Yoshihiro Makide of the University of Tokyo for his assistance in setup and equipment support for the field analytical laboratory. We also thank Captain Gary Marsten of U.S. Air Force and the personnel of the Yokota Air Base for the use of laboratory space, liquid nitrogen supply, and the logistic support in transporting and shipping canisters between Yokota and the various staging sites. Merged data sets provided by S. Sandholm and J. Bradshaw of Georgia Tech were invaluable in the construction and comparison of contour plots. John Bilicska carried out the difficult and time consuming task of developing the color patch plotting program and

generating the color plots. This work was supported by funds from the National Aeronautics and Space Administration (NASA) grant NAG-1-783 and the W.M. Keck Foundation.

References

Atkinson, R., Gas-phase tropospheric chemistry of organic compounds: A review, *Atmos. Environ., 24* (A) 1-44, 1990.

Bachmeier, A. S., R. E. Newell, M. C. Shipham, Y. Zhu, D. R. Blake, and E. V. Browell, PEM-W A: Meteorological overview, *J. Geophys. Res.*, this issue.

Blake, D. R., D. F. Hurst, T. W. Smith Jr., W. J. Whipple, T.-Y. Chen, N. J. Blake, and F. S. Rowland, Summertime measurements of selected nonmethane hydrocarbons in the Arctic and subarctic during the 1988 Arctic Boundary Layer Expedition (ABLE 3A), *J. Geophys. Res. 97*, 16559, 1992.

Blake, D. R., T. W. Smith Jr., T.-Y. Chen, W. J. Whipple and F. S. Rowland, Effects of biomass burning on summertime nonmethane hydrocarbon concentrations in the Canadian wetlands, *J. Geophys. Res., 99*, 1699, 1994.

Blake, D. R. and F. S. Rowland, Urban leakage of liquefied petroleum gas and its impact on Mexico City Air Quality, *Science, 269*, 953-956, 1995.

Bonsang, B., D. Martin, G. Lambert, M. Kanakidou, J. C. Le Roulley, and G. Sennequier, Vertical distribution of nonmethane hydrocarbons in the remote marine boundary layer, *J. Geophys. Res., 96*, 7313, 1991.

Collins, J. E., Jr., G. W. Sachse, B. E. Anderson, R. C. Harriss, S. Sandholm, L. O. Wade, L. G. Burney, and G. F. Hill, Airborne nitrous oxide observations over the western Pacific Ocean: September-October 1991, *J. Geophys. Res.*, this issue.

Crutzen, P. J. in *Atmospheric Chemistry*, The atmospheric sciences: National objectives for the 1980's; Natl. Res. Council, Washington, D. C., 1980.

Crutzen, P. J. and M. O. Andreae, Biomass burning in the tropics: Impact on atmospheric chemistry and biogeochemical cycles, *Science, 250*, 1669, 1990.

DeMore, W. B., S. P. Sander, D. M. Golden, R. F. Hampson, M. J. Kurylo, C. J. Howard, A. R. Ravishankara, C. E. Kolb, and M. J. Molina, Chemical kinetics and photochemical data for use in stratospheric modeling, in *Evaluation 10, JPL Publ. 92-20* NASA Jet Propul. Lab., Pasadena, Calif., 1992.

Dickerson, R. R., et al., Thunderstorm: An important mechanism in the transport of air pollutants, *Science, 235*, 460, 1987.

Ehhalt, D. H., Concentrations and distributions of atmospheric trace gases, *Ber. Bunsenges. Phys. Chem., 96*, 1992.

Ehhalt, D. H. and J. Rudolph, On the importance of light hydrocarbons in multiphase atmospheric systems, *Ber. Kernforschungsanlage Jülich, JÜL-1942*, pp. 1-43, 1984.

Ehhalt, D. H., J. Rudolph, F. Meixner, and U. Schmidt, Measurements of selected C2-C5 hydrocarbons in the background troposphere: Vertical and latitudinal variations, *J. Atmos. Chem., 3*, 29, 1985.

Greenberg, J. P, P. R. Zimmerman, and P. Haagenson, Tropospheric hydrocarbons and CO profiles over the U.S. west coast of Alaska, *J. Geophys. Res., 95*, 14,105, 1990.

Hough, A. M., Development of a two-dimensional global tropospheric model: Model chemistry, *J. Geophys. Res.*, 96, 7325, 1991.

Merrill, J. T., Trajectory results and interpretation for PEM-West A, *J. Geophys. Res.*, this issue.

Newell, R. E, et al., Atmospheric sampling of supertyphoon Mireille with the NASA DC-8 aircraft on September 27, 1991, during PEM-West A, *J. Geophys. Res.*, this issue.

Prinn, R., et al., Global average concentration and trend for hydroxyl radicals reduced from ALE/GAGE trichloroethane (methyl chloroform) data for 1978-1990, *J. Geophys. Res., 97*, 2445-2461, 1992.

Rasmussen, R. A., M. A. K. Khalil, and J. S. Chang, Atmospheric trace gases over China, *Environ. Sci. Technol. 16*, 124, 1982.

Rudolph, J., Two-dimensional distribution of light hydrocarbons: Results from the STRATOZ III experiment, *J. Geophys. Res., 93*, 8367, 1988.

Singh, H. B., Viezee, and L. J. Salas, Measurements of selected C_2-C_5 hydrocarbons in the troposphere: Latitudinal, vertical, and temporal variations, *J. Geophys. Res., 93*, 15861, 1988.

Smith, T. W., Jr., Summertime tropospheric nonmethane hydrocarbon and halocarbon concentrations over central and eastern Canada during ABLE-3B, Ph.D. thesis, Univ. of Calif., Irvine, 1993.

Talbot, B. et al., Chemical characteristics of continental outflow from Asia to the troposphere over the western Pacific Ocean during September-October 1991: Results from PEM-WEST A,, *J. Geophys. Res.*, this issue.

World Meteorological Organization (WMO), Scientific assessment of ozone depletion: 1991, WMO Rep. 25, UNEP, Geneva, 1992.

Donald R. Blake, Tai-Yih Chen, Tyrrel W. Smith, Jr., Charles J.-L. Wang, Oliver W. Wingenter, Nicola J. Blake, and F. S. Rowland, Department of Chemistry, University of California, Irvine. (email: dblake@orion.oac.uci.edu; tchen@orion.oac.uci.edu; Ty@terra.colorado.edu; cwang@sparc20.ncu.edu.tw; owwingen@uci.edu; nblake@orion.oac.uci.edu; rowland@uci.edu)

Edward W. Mayer, Department of Chemistry, U.S. Military Academy, West Point, New York. (email: emayer@chem.ucsd.edu)

Ty(email: ty@terra.colorado.edu)

(Received June 28, 1994; revised June 13, 1995; accepted June 18, 1995.)